

**Electronic Supplementary Information:**

**Through-Space Charge Transfer within Single-Component Organic**

**Crystal: Visual Detection and Rational Regulation**

Zhenjiang Liu<sup>a</sup>, Jia Ren<sup>a</sup>, Hui Zhang<sup>a</sup>, Yunsheng Wang<sup>ab</sup>, Xiaoning Li<sup>a</sup>, Jiaqiang Wang<sup>a</sup>, Manman Fang<sup>a</sup>, Jie Yang<sup>a\*</sup>,  
Ben Zhong Tang<sup>ac\*</sup>, Zhen Li<sup>abd\*</sup>

<sup>a</sup> Institute of Molecular Aggregation Science, Tianjin University, Tianjin 300072, China. E-mail: jieyang2018@tju.edu.cn

<sup>b</sup> Joint School of National University of Singapore, Tianjin University, International Campus of Tianjin University, Binhai New City, Fuzhou, 350207, China.

<sup>c</sup> Shenzhen Institute of Molecular Aggregate Science and Engineering, School of Science and Engineering, The Chinese University of Hong Kong, Shenzhen, Guangdong, 518172, China. E-mail: tangbenz@cuhk.edu.cn.

<sup>d</sup> Hubei Key Lab on Organic and Polymeric Opto-Electronic Materials, Department of Chemistry, Wuhan University, Wuhan, 430072, China. E-mail: lizhen@whu.edu.cn.

## Table of contents

### 1. Experimental Procedures

**Scheme S1** Chemical structures of PtzO, BP, PtzO-CH<sub>3</sub>, BP-OH and general procedure for the synthesis of PtzO-nC-BP (n = 3-6).

**Scheme S2** The detailed synthetic route of BP-nC-Br (n = 3-6).

**Scheme S3** The detailed synthetic route of Ptz-nC-BP (n = 3-6).

**Scheme S4** The detailed synthetic route of PtzO-nC-BP (n = 3-6).

### 2. Results and Discuss

**Chart S1** Schematic illustration of D- $\pi$ -A structure and through-space charge transfer (TSCT) to realize high photoluminescence quantum yield (PLQY) of TADF. Copyright 2020, Nature Publishing Group.

**Chart S2** Exciplex fluorescence emission based on intermolecular CT interaction in multicomponent system. Copyright 2012, Nature Publishing Group.

**Chart S3** Red-shifted fluorescence emission in co-crystal system due to space charge transfer. Copyright 2017, Wiley-VCH.

**Chart S4** (a) RTP emission based on intermolecular CT effect between carbazole (Cz) and 1*H*-benzo[*f*]indole (Bd). (b) Efficient RTP emission of bicomponent doping system based on intermolecular CT between 4BBI and 1BBI. Copyright 2020, Nature Publishing Group; Copyright 2020, The American Association for the Advancement of Science.

**Chart S5** High RTP efficiency and long afterglow emission based on intermolecular CT in M-CH<sub>3</sub> and M-C<sub>2</sub>H<sub>5</sub>. Copyright 2021, Wiley-VCH.

**Figure S1** High performance liquid chromatography diagrams of PtzO-nC-BP (n = 3-6).

**Figure S2** <sup>1</sup>H NMR spectrum of PtzO-3C-BP.

**Figure S3** <sup>13</sup>C NMR spectrum of PtzO-3C-BP.

**Figure S4** <sup>1</sup>H NMR spectrum of PtzO-4C-BP.

**Figure S5** <sup>13</sup>C NMR spectrum of PtzO-4C-BP.

**Figure S6** <sup>1</sup>H NMR spectrum of PtzO-5C-BP.

**Figure S7** <sup>13</sup>C NMR spectrum of PtzO-5C-BP.

**Figure S8** <sup>1</sup>H NMR spectrum of PtzO-6C-BP.

**Figure S9** <sup>13</sup>C NMR spectrum of PtzO-6C-BP.

**Figure S10** Thermo-gravimetric analysis (TGA) curves of PtzO-nC-BP (n = 3-6).

**Figure S11** Differential scanning calorimeter (DSC) curves of PtzO-nC-BP (n = 3-6).

**Figure S12** Phosphorescence decay curves of PtzO-CH<sub>3</sub>, BP-OH and PtzO-CH<sub>3</sub> + BP-OH (molar ratio 1:1) in solution state at 77 K ( $\lambda_{\text{ex}}$  = 330 nm, 10  $\mu$ M).

**Figure S13** Phosphorescence spectra of PtzO-CH<sub>3</sub> and BP-OH in solution state at 77 K ( $\lambda_{\text{ex}}$  = 330 nm; 10  $\mu$ M same slit: ex5-em5).

**Figure S14** Photographs of PtzO-nC-BP (n = 3-6) taken at different time, before and after the removal of UV excitation.

**Figure S15** (a) Phosphorescence spectra of PtzO-3C-BP crystal at 77 K ( $\lambda_{\text{ex}}$  = 330 nm). (b) Phosphorescence decay curve of PtzO-3C-BP crystal at 450 nm under 77 K. (c) Phosphorescence decay curve of PtzO-3C-BP crystal at 530nm under 77 K.

**Figure S16** CV curves of PtzO-CH<sub>3</sub> and BP-OH.

**Table S1** Calculated energy levels of PtzO-CH<sub>3</sub> and BP-OH

**Figure S17** Schematic diagram of exciplex formation.

**Figure S18** Phosphorescence excitation spectra of PtzO-CH<sub>3</sub>, BP-OH, their mixture and PtzO-3C-BP in DCM solution states (10  $\mu$ M) at 77 K and PtzO-3C-BP in crystal state at room temperature.

**Figure S19** PXRD patterns for PtzO-3C-BP in crystal state and grinding state, and simulation PXRD pattern based on its single crystal data, respectively.

**Figure S20** (a) Phosphorescence spectra of PtzO-3C-BP crystal before and after heavy grinding for 10 min at room temperature ( $\lambda_{\text{ex}}$  = 365 nm). (b) Phosphorescence decay curves of PtzO-3C-BP crystal after heavy grinding for 10 min at room temperature ( $\lambda_{\text{ex}}$  = 365 nm). (Greater sensitivity of CT phosphorescence to molecular packing)

**Table S2** Single crystal structure data of PtzO-3C-BP.

**Figure S21** Schematic illustration of D-A packing in PtzO-3C-BP crystal.

**Figure S22** Local packing of PtzO-3C-BP crystal, in which no  $\pi$ - $\pi$  stacking was formed by adjacent phenothiazine 5,5-dioxide units.

**Figure S23** Phosphorescence spectra of PtzO-3C-BP with different concentrations in DCM solution at 77 K ( $\lambda_{\text{ex}}$  = 330 nm).

**Figure S24** (a) Phosphorescence spectra of PtzO-CH<sub>3</sub> + BP-OH solid mixture (molar ratio 1:1) and PtzO-CH<sub>3</sub> crystal and (b) BP-OH crystal at room temperature ( $\lambda_{\text{ex}}$  = 365 nm).

**Figure S25** (a) Phosphorescence decay curves of PtzO-CH<sub>3</sub> + BP-OH solid mixture (molar ratio 1:1) and PtzO-CH<sub>3</sub> crystal and

(b) BP-OH crystal at room temperature ( $\lambda_{\text{ex}} = 365 \text{ nm}$ ).

**Figure S26** PXRD patterns for Ptzo-CH<sub>3</sub> + BP-OH solid mixture and individual powders of Ptzo-CH<sub>3</sub> and BP-OH, respectively.

**Figure S27** (a) UV-Vis absorption spectra of Ptzo-nC-BP ( $n = 3-6$ ) in dichloromethane (DCM) solution ( $10 \mu\text{M}$ ). (b) Steady-state PL spectra of Ptzo-nC-BP ( $n = 3-6$ ) in DCM solution ( $10 \mu\text{M}$ ) at 77 K ( $\lambda_{\text{ex}} = 330 \text{ nm}$ ). (c) Phosphorescence spectra of Ptzo-nC-BP ( $n = 3-6$ ) in DCM solution ( $10 \mu\text{M}$ ) at 77 K ( $\lambda_{\text{ex}} = 330 \text{ nm}$ ). (d) Corresponding time-resolved phosphorescence decay curves of Ptzo-nC-BP ( $n = 3-6$ ) in DCM solution ( $10 \mu\text{M}$ ) at 77 K ( $\lambda_{\text{ex}} = 330 \text{ nm}$ ).

**Figure S28** Steady-state PL spectra of Ptzo-nC-BP ( $n = 3-6$ ) in DCM solution ( $10 \mu\text{M}$ ) at room temperature ( $\lambda_{\text{ex}} = 330 \text{ nm}$ ).

**Figure S29** UV-Vis absorption spectra of Ptzo-nC-BP ( $n = 4-6$ ) in crystal state at room temperature

**Figure S30** Excitation-phosphorescence mappings of Ptzo-nC-BP ( $n = 4-6$ ) in crystal state at room temperature.

**Figure S31** Time-resolved RTP decay curves of Ptzo-4C-BP crystal at (a) 450 nm and (b) 520 nm ( $\lambda_{\text{ex}} = 365 \text{ nm}$ ).

**Figure S32** Time-resolved RTP decay curves of Ptzo-5C-BP crystal at (a) 450 nm and (b) 520 nm ( $\lambda_{\text{ex}} = 365 \text{ nm}$ ).

**Figure S33** Time-resolved RTP decay curves of Ptzo-6C-BP crystal at (a) 450 nm and (b) 520 nm ( $\lambda_{\text{ex}} = 365 \text{ nm}$ ).

**Figure S34** Steady-state PL spectra of Ptzo-nC-BP ( $n = 3-6$ ) in crystal state at room temperature.

**Figure S35** Phosphorescence spectra of Ptzo-nC-BP ( $n = 4-6$ ) crystals at 77 K.

**Figure S36** (a) Phosphorescence decay curve of Ptzo-4C-BP crystal at 450 nm under 77 K. (b) Phosphorescence decay curve of Ptzo-4C-BP crystal at 530nm under 77 K. (c) Phosphorescence decay curve of Ptzo-5C-BP crystal at 450 nm under 77 K. (d) Phosphorescence decay curve of Ptzo-5C-BP crystal at 530nm under 77 K. (e) Phosphorescence decay curve of Ptzo-6C-BP crystal at 450 nm under 77 K. (f) Phosphorescence decay curve of Ptzo-6C-BP crystal at 530nm under 77 K.

**Table S3** Single crystal data of Ptzo-nC-BP ( $n = 4-6$ ).

**Figure S37** Schematic illustration of D-A packing in Ptzo-nC-BP ( $n = 4-6$ ) crystals.

**Figure S38** The analyses of phosphorescence band and corresponding intensity of (a) Ptzo-3C-BP crystal, (b) Ptzo-4C-BP crystal, (c) Ptzo-5C-BP crystal and (d) Ptzo-6C-BP crystal at room temperature.

**Table S4** RTP performance of Ptzo-nC-BP ( $n = 3-6$ ) crystals at room temperature and the distance between N and O in D-A pairs.

## 1. Experimental Procedures

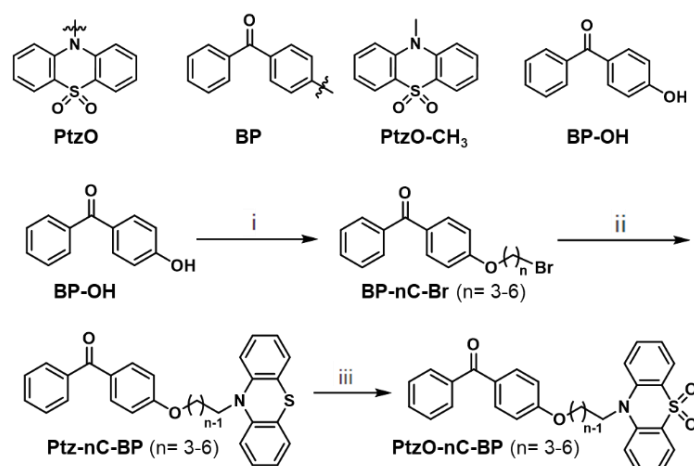
### Supplementary Methods

**General**  $^1\text{H}$  NMR and  $^{13}\text{C}$  NMR spectra were recorded on a 400 MHz Bruker AVANCE III spectrometer using  $\text{CDCl}_3$  as solvent. Mass spectra were measured on a UHPLC/Q-TOF MS spectrophotometer. High-performance liquid chromatogram spectra were recorded on Agilent 1100 HPLC. Thermo-gravimetric analysis curves and differential scanning calorimeter curves were recorded on Thermo Gravimetric Analysis TG-209F3 and Differential Scanning Calorimeter DSC214 ployma. UV-Vis spectra were measured on a Shimadzu UV-2600. Photoluminescence spectra were performed on a Hitachi F-4600 fluorescence spectrophotometer in air. Phosphorescence lifetimes, photoluminescence quantum yields and fluorescence lifetimes were determined with FLS1000 spectrometer in air. The single-crystal X-ray diffraction data of these samples were collected in XtaLAB SuperNova X-ray diffractometer. Powder X-ray diffraction (PXRD) patterns were recorded by Rigaku Smartlab9KW.

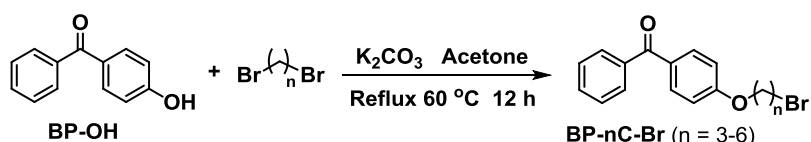
The Gaussian 09 program was utilized to perform the TD-DFT calculations. The HOMO/LUMO orbital distributions were evaluated by the TD-m062x/6-31g\*.

In this study, when we refer to 'solution' measurements at 77 K, it is indeed in the context of a frozen DCM matrix. The term 'solution' is used in a broader sense to indicate the initial state of the sample before cooling. As the temperature is lowered to 77 K, DCM translates into a solid phase, effectively creating a rigid environment for this system.

### Synthesis

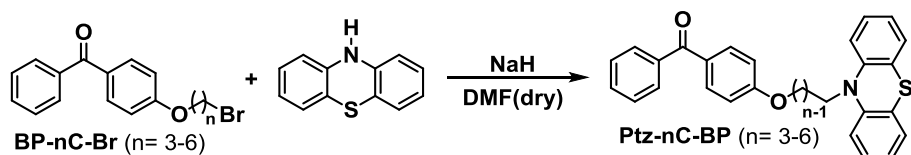


**Scheme S1** Chemical structures of PtzO, BP, PtzO-CH<sub>3</sub>, BP-OH and general procedure for the synthesis of PtzO-nC-BP (n = 3-6).



**Scheme S2** The detailed synthetic route of BP-nC-Br (n = 3-6).

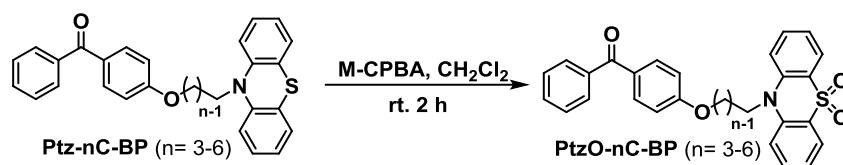
(i) BP-nC-Br (n = 3-6): Compound BP-OH (2 g, 10.1 mmol) was added to a suspension of potassium carbonate ( $\text{K}_2\text{CO}_3$ ) (2.8 g, 20.2 mmol) in acetone solution (30 mL), and stirred for 30 min at 60 °C. Then, 1, n-dibromo alkane (n = 3-6) (12 mmol) was added dropwise to the mixture and refluxed at 60 °C. After 12 h, the color of this solution changed from yellow to transparent. The crude product was concentrated by rotary evaporation and then purified by column chromatography on silica gel using petroleum ether (PE)/dichloromethane (DCM) (5:1 v/v) as eluent. Finally, white solids with yields in the range of 92%~97% were obtained.



**Scheme S3** The detailed synthetic route of Ptz-nC-BP (n = 3-6).

(ii) Ptz-nC-BP (n = 3-6): Phenothiazine (2.2 g, 11 mmol) was added to an ice-cooled suspension of NaH (60% in mineral oil, 0.6 g, 15 mmol) in dry N,N-dimethylformamide (DMF) solution (30 mL), and stirred for 30 min under N<sub>2</sub>. Then, BP-nC-Br (10 mmol) was added dropwise and the mixture was stirred at 0 °C under N<sub>2</sub>. After 4 h, water was added to the mixture to quench this reaction. The organic layer was collected with DCM and dried over by anhydrous Na<sub>2</sub>SO<sub>4</sub> and concentrated by

rotary evaporation. The crude product was purified by column chromatography on silica gel using PE/DCM/ethyl acetate (EA) (5:5:1 v/v/v) as eluent. Finally, white solids with yields in the range of 88%~93% were obtained.



**Scheme S4** The detailed synthetic route of PtzO-nC-BP (n= 3-6).

(iii) PtzO-nC-BP (n= 3-6): 3-Chloroperbenzoic acid (M-CPBA) (2.6 g, 15 mmol) was added to a suspension of Ptz-nC-BP (6 mmol) in DCM solution (20 mL). The mixture was stirred for 2 h at room temperature, then neutralized with a solution of sodium hydroxide to remove excess M-CPBA. The organic layer was collected with DCM and dried over by anhydrous  $\text{Na}_2\text{SO}_4$  and concentrated by rotary evaporation. The crude product was purified by column chromatography on silica gel using PE/DCM/EA (5:5:2 v/v/v) as eluent. Finally, white solids with yields in the range of 90%~94% were obtained.

PtzO-3C-BP: White solid. mp: 178.7 °C;  $^1\text{H}$  NMR (400 MHz,  $\text{CDCl}_3$ ):  $\delta$  8.09 (d,  $J$  = 8.0 Hz, 2H), 7.75 (q,  $J$  = 8.8 Hz, 4H), 7.57 (m, 3H), 7.46 (t,  $J$  = 9.6 Hz, 4H), 7.25 (t,  $J$  = 3.6 Hz, 2H), 6.91 (d,  $J$  = 7.2 Hz, 2H), 4.49 (t,  $J$  = 7.2 Hz, 2H), 4.14 (t,  $J$  = 5.2 Hz, 2H), 2.37 (m, 2H);  $^{13}\text{C}$  NMR (100 MHz,  $\text{CDCl}_3$ ):  $\delta$  195.61, 162.11, 141.10, 138.22, 133.23, 132.65, 132.08, 130.53, 129.84, 128.30, 125.13, 123.79, 122.21, 116.29, 114.10, 64.67, 44.36, 26.90; HRMS (ESI),  $m/z$ :  $[\text{M}+\text{Na}]^+$  calcd. for  $\text{C}_{28}\text{H}_{23}\text{NNaO}_4\text{S}$ , 492.1243; found, 492.1240.

PtzO-4C-BP: White solid. mp: 163.4 °C;  $^1\text{H}$  NMR (400 MHz,  $\text{CDCl}_3$ ):  $\delta$  8.11 (dd,  $J_1$  = 8.0 Hz,  $J_2$  = 1.6 Hz, 2H), 7.80 (d,  $J$  = 8.8 Hz, 2H), 7.74 (d,  $J$  = 6.8 Hz, 2H), 7.57 (m, 3H), 7.46 (t,  $J$  = 6.8 Hz, 2H), 7.37 (d,  $J$  = 8 Hz, 2H), 7.27 (t,  $J$  = 6.4 Hz, 2H), 6.92 (d,  $J$  = 8.8 Hz, 2H), 4.30 (t,  $J$  = 7.2 Hz, 2H), 4.09 (t,  $J$  = 6 Hz, 2H), 2.14 (m, 2H), 1.95 (m, 2H).  $^{13}\text{C}$  NMR (100 MHz,  $\text{CDCl}_3$ ):  $\delta$  195.61, 162.39, 141.07, 138.27, 133.21, 132.71, 132.05, 130.41, 129.82, 128.30, 124.84, 123.81, 122.08, 116.20, 114.04, 67.40, 47.74, 26.01, 23.76; HRMS (ESI),  $m/z$ :  $[\text{M}+\text{Na}]^+$  calcd. for  $\text{C}_{29}\text{H}_{25}\text{NNaO}_4\text{S}$ , 506.1382; found, 506.1397.

PtzO-5C-BP: White solid. mp: 140.8 °C;  $^1\text{H}$  NMR (400 MHz,  $\text{CDCl}_3$ ):  $\delta$  8.11 (dd,  $J_1$  = 8.0 Hz,  $J_2$  = 1.6 Hz, 2H), 7.80 (dt,  $J_1$  = 2.8 Hz,  $J_2$  = 9.2 Hz, 2H), 7.74 (dd  $J_1$  = 8.4 Hz,  $J_2$  = 1.6 Hz, 2H), 7.59 (m, 3H), 7.47 (t,  $J$  = 7.6 Hz, 2H), 7.34 (d,  $J$  = 8.4 Hz, 2H), 7.26 (t,  $J$  = 7.6 Hz, 2H), 6.92 (dt,  $J_1$  = 6.8 Hz,  $J_2$  = 2 Hz, 2H), 4.22 (t,  $J$  = 7.6 Hz, 2H), 4.04 (t,  $J$  = 6 Hz, 2H), 2.00 (m, 2H), 1.87 (m, 2H), 1.65 (m, 2H).  $^{13}\text{C}$  NMR (100 MHz,  $\text{CDCl}_3$ ):  $\delta$  195.66, 162.66, 141.05, 138.33, 133.21, 132.68, 132.02, 130.18, 129.82, 128.30, 124.69, 123.77, 122.00, 116.17, 114.07, 67.88, 48.09, 28.74, 26.69, 23.31. HRMS (ESI),  $m/z$ :  $[\text{M}+\text{Na}]^+$  calcd. for  $\text{C}_{30}\text{H}_{27}\text{NNaO}_4\text{S}$ , 520.1555; found, 520.1553.

PtzO-6C-BP: White solid. mp: 130.8 °C;  $^1\text{H}$  NMR (400 MHz,  $\text{CDCl}_3$ ):  $\delta$  8.11 (dd,  $J_1$  = 8.0 Hz,  $J_2$  = 1.6 Hz, 2H), 7.80 (d,  $J$  = 8.8 Hz, 2H), 7.74 (dd  $J_1$  = 8.4 Hz,  $J_2$  = 1.6 Hz, 2H), 7.58 (m, 3H), 7.46 (t,  $J$  = 7.6 Hz, 2H), 7.33 (d,  $J$  = 8.4 Hz, 2H), 7.26 (t,  $J$  = 7.2 Hz, 2H), 6.92 (d,  $J$  = 8.8 Hz, 2H), 4.19 (t,  $J$  = 7.2 Hz, 2H), 4.02 (t,  $J$  = 6.4 Hz, 2H), 1.95 (m, 2H), 1.83 (m, 2H), 1.54 (m, 4H).  $^{13}\text{C}$  NMR (100 MHz,  $\text{CDCl}_3$ ):  $\delta$  195.67, 162.77, 141.02, 138.36, 133.18, 132.68, 131.99, 130.10, 129.82, 128.29, 124.59, 123.79, 121.95, 116.10, 114.07, 100.00, 67.95, 48.17, 29.09, 26.87, 26.40, 25.78. HRMS (ESI),  $m/z$ :  $[\text{M}+\text{Na}]^+$  calcd. for  $\text{C}_{31}\text{H}_{29}\text{NNaO}_4\text{S}$ , 534.1714; found, 534.1710.

### Crystal culture and structure

The single crystals were cultured by slow solvent evaporation under the same conditions. PtzO-nC-BP (n = 3-6) (5 mg) was dissolved in good solvent of dichloromethane (DCM) (2 mL), followed by adding with poor one of petroleum ether (PE) (5 mL) to it. Then the bottle was sealed with tin foil and several small holes were poked in the tin foil by 5 mL syringe needle. Through slow solvent evaporation after about a week, transparent block crystals suitable for X-ray diffraction analysis were obtained. The structural analysis was conducted using OLEX2, with initial solutions obtained through the SHELXT program and refinements performed via full-matrix least squares on F-squared. The supplementary Crystallographic Information Files (CIFs), including structure factors, can be accessed through the Cambridge Crystallographic Data Centre (CCDC).

## 2. Results and Discussion

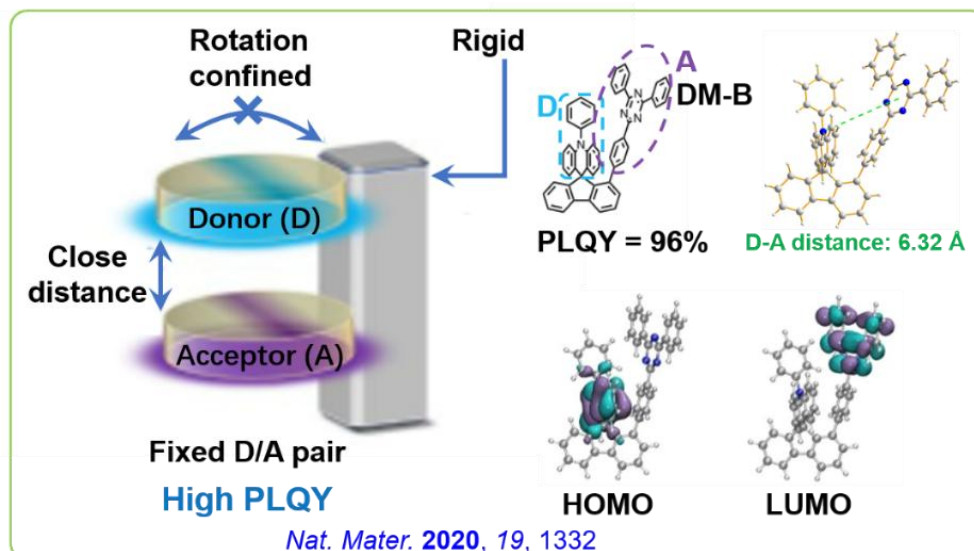


**Chart S1** Schematic illustration of D- $\pi$ -A structure and through-space charge transfer (TSCT) to realize high photoluminescence quantum yield (PLQY) of TADF. Copyright 2020, Nature Publishing Group.

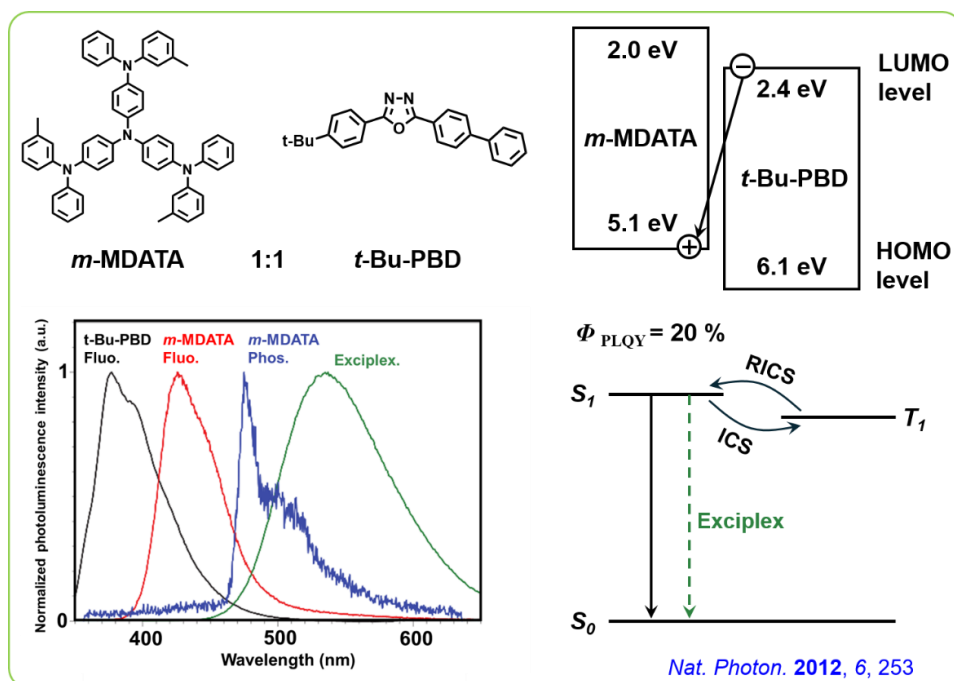


**Chart S2** Exciplex fluorescence emission based on intermolecular CT interaction in multicomponent system. Copyright 2012, Nature Publishing Group.

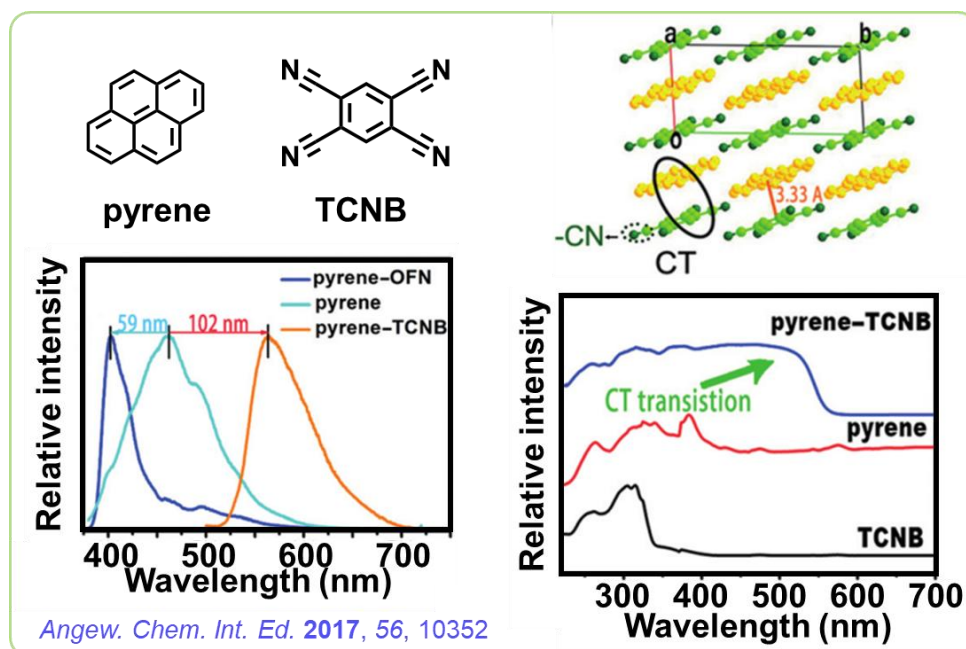


Chart S3 Red-shifted fluorescence emission in co-crystal system due to space charge transfer. Copyright 2017, Wiley-VCH.

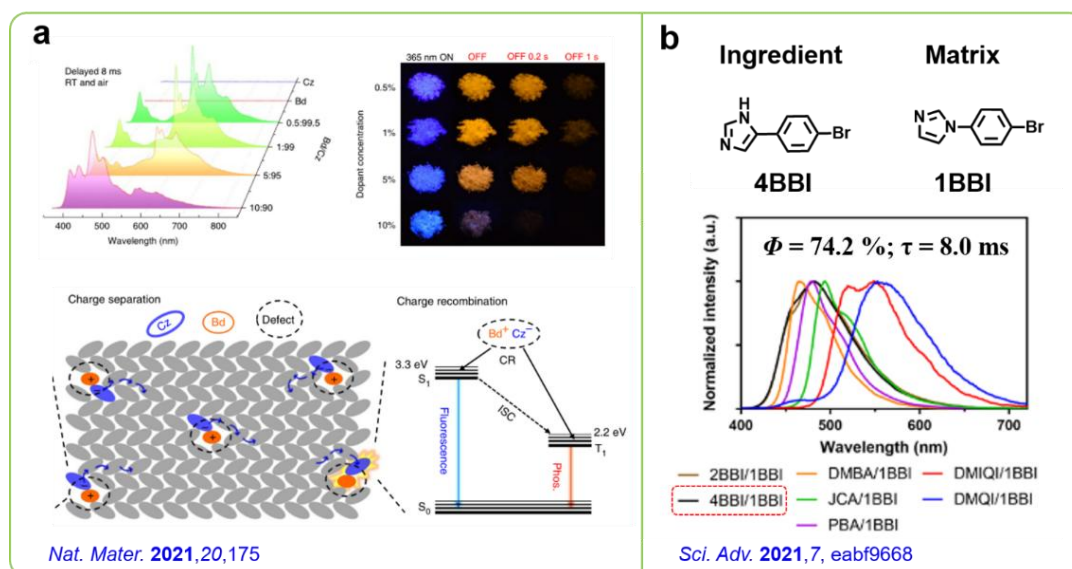
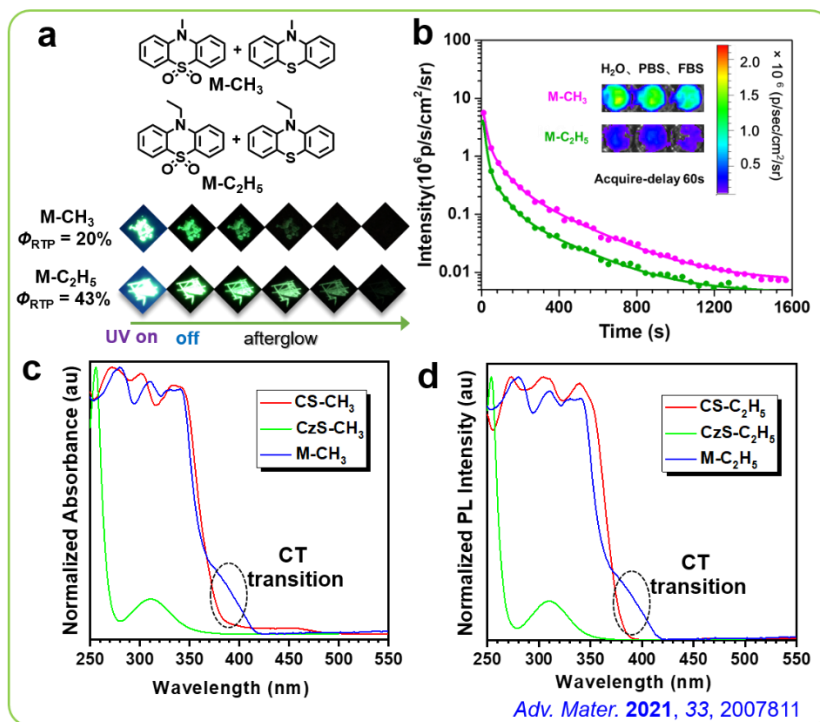
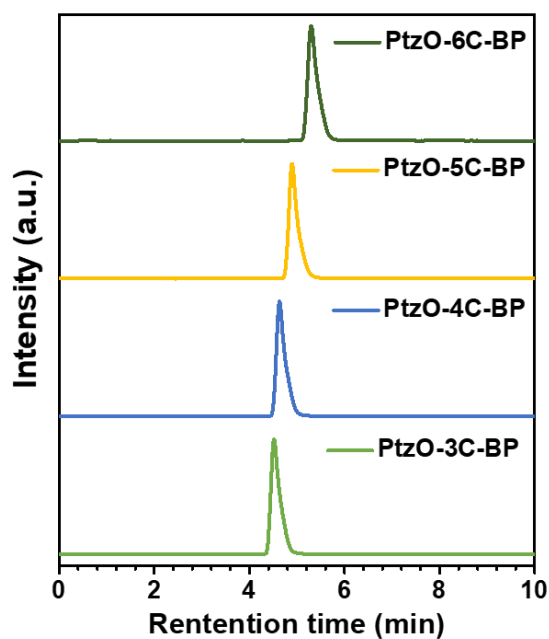


Chart S4 (a) RTP emission based on intermolecular CT effect between carbazole (Cz) and 1H-benzof[j]indole (Bd). (b) Efficient RTP emission of bicomponent doping system based on intermolecular CT between 4BBI and 1BBI. Copyright 2020, Nature Publishing Group; Copyright 2020, The American Association for the Advancement of Science.



**Chart S5** High RTP efficiency and long afterglow emission based on intermolecular CT in M-CH<sub>3</sub> and M-C<sub>2</sub>H<sub>5</sub>. Copyright 2021, Wiley-VCH.



**Figure S1** High performance liquid chromatography diagrams of PtZO-nC-BP (n = 3-6).

Note: The chromatographic analysis employs a CS C18 reversed-phase column with specification of 5  $\mu$ m particle size and dimension of 4.6 mm by 150 mm. Acetonitrile serves as the mobile phase, maintained at a flow rate of 1 mL min<sup>-1</sup>. Detection is carried out at a wavelength of 254 nm and the column temperature is controlled at 298 K.



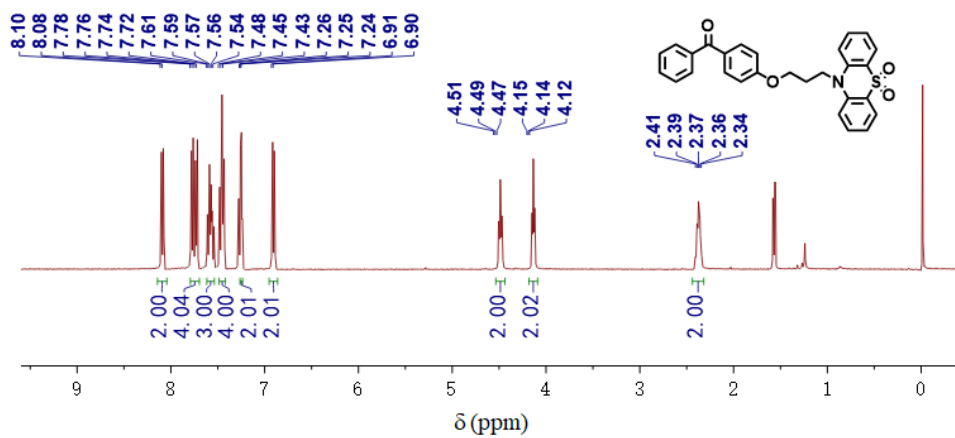


Figure S2  $^1\text{H}$  NMR spectrum of PtzO-3C-BP.

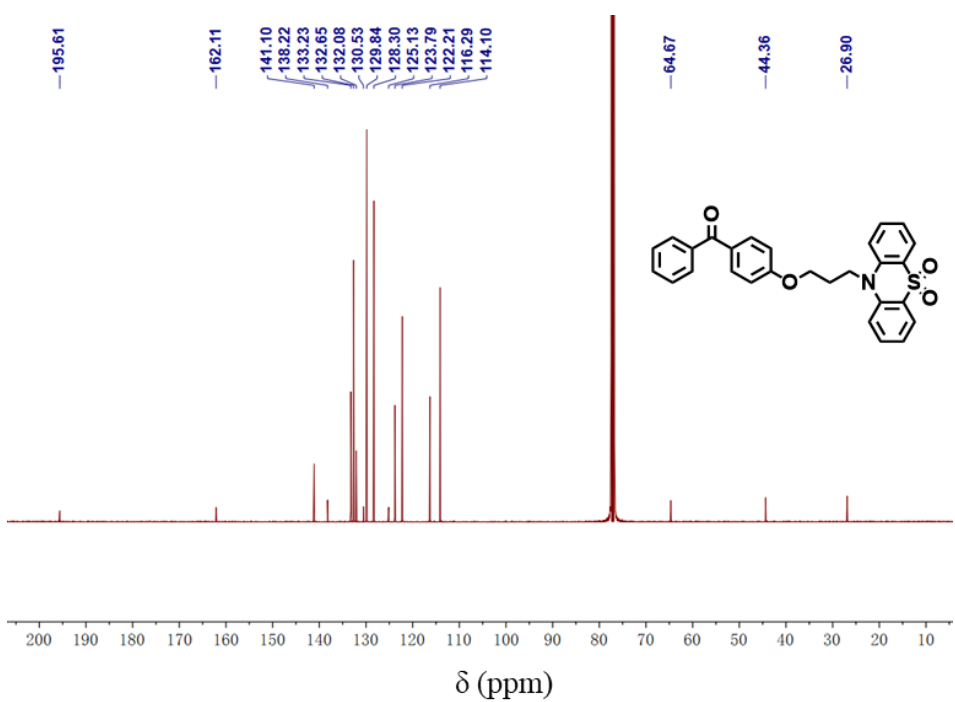


Figure S3  $^{13}\text{C}$  NMR spectrum of PtzO-3C-BP.

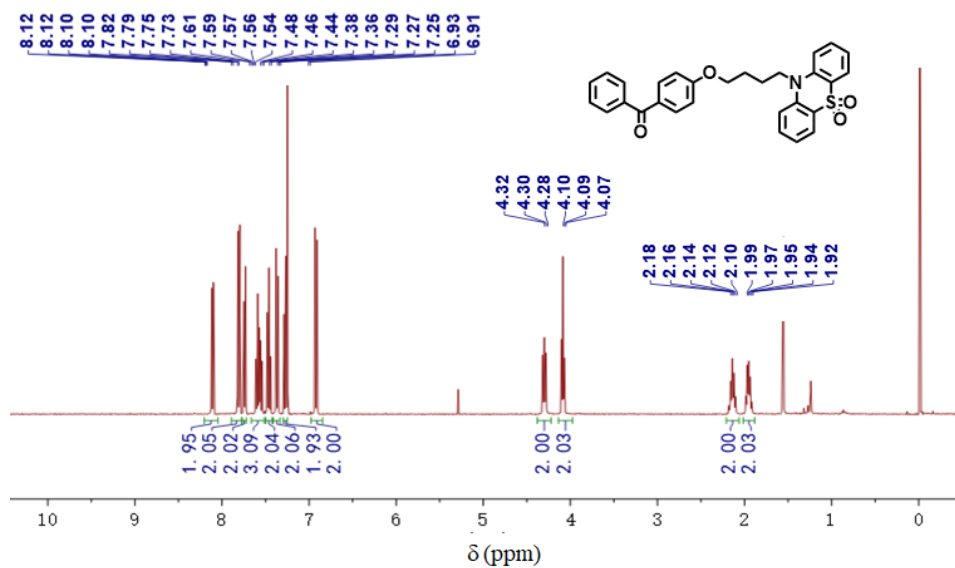


Figure S4  $^1\text{H}$  NMR spectrum of PtzO-4C-BP.

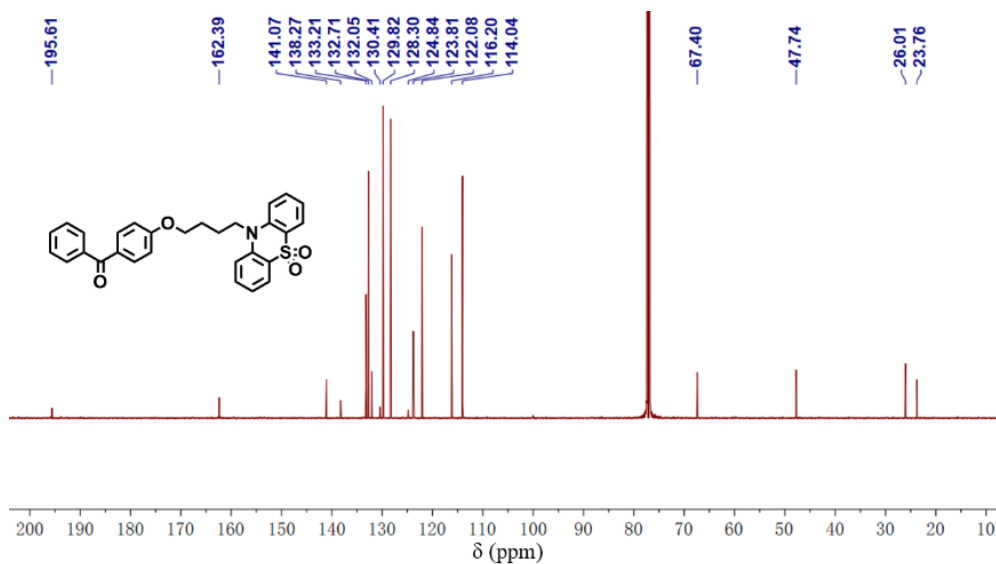


Figure S5  $^{13}\text{C}$  NMR spectrum of PtzO-4C-BP.

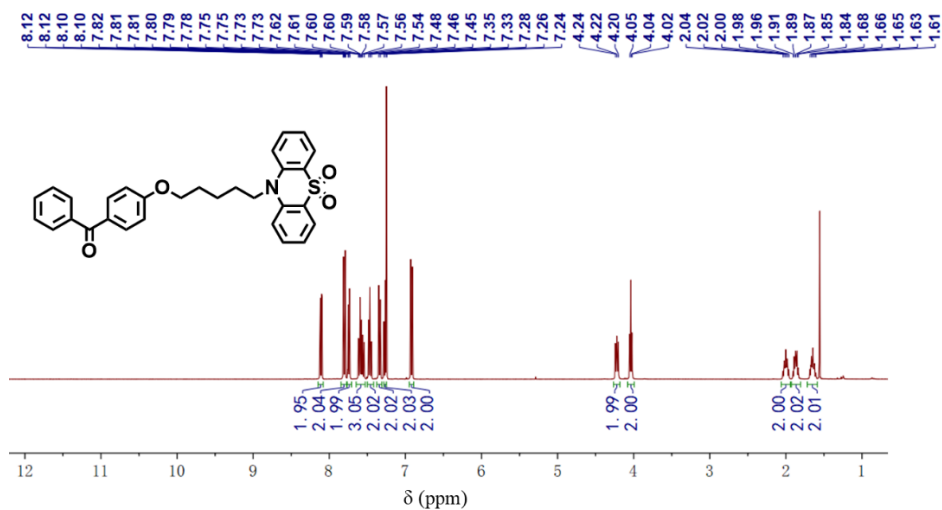


Figure S6 <sup>1</sup>H NMR spectrum of PtzO-5C-BP.

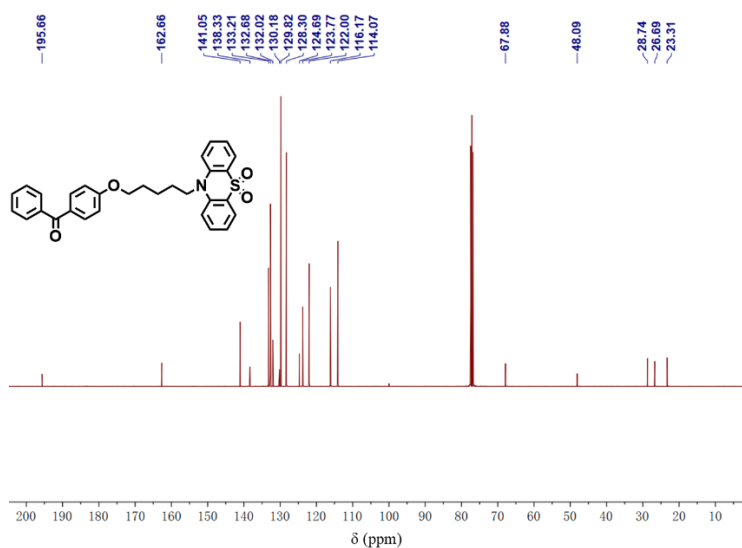


Figure S7 <sup>13</sup>C NMR spectrum of PtzO-5C-BP.

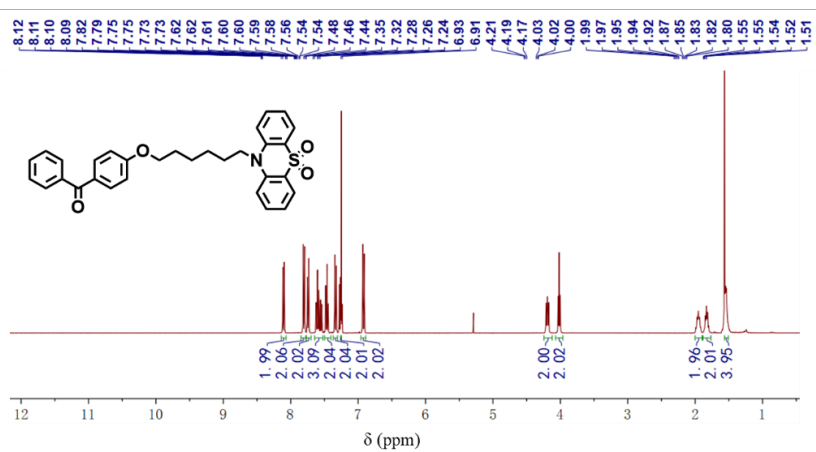


Figure S8 <sup>1</sup>H NMR spectrum of PtzO-6C-BP.

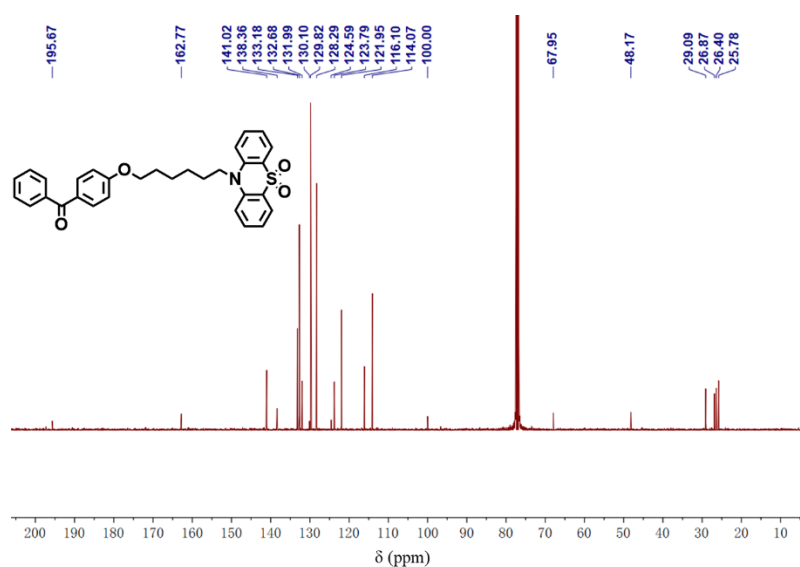


Figure S9  $^{13}\text{C}$  NMR spectrum of Ptzo-6C-BP.

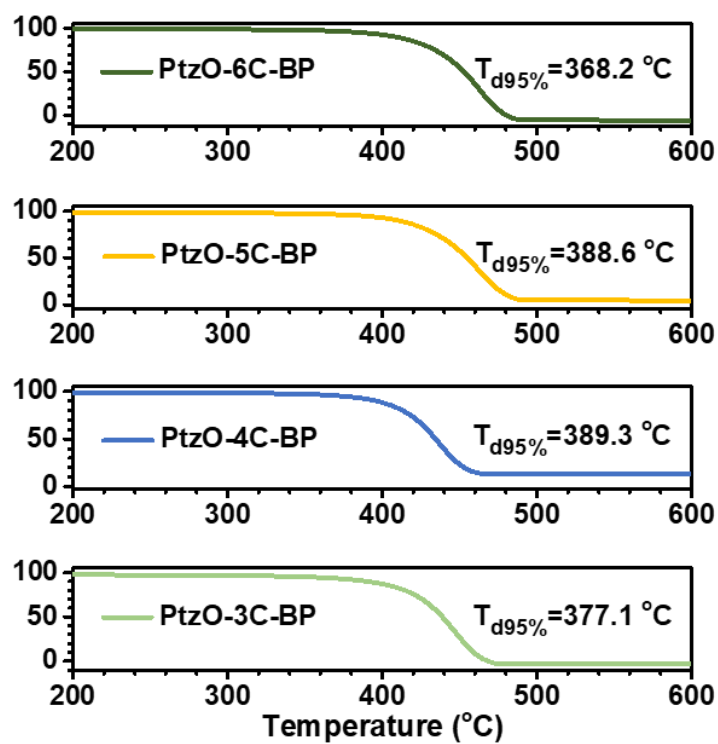
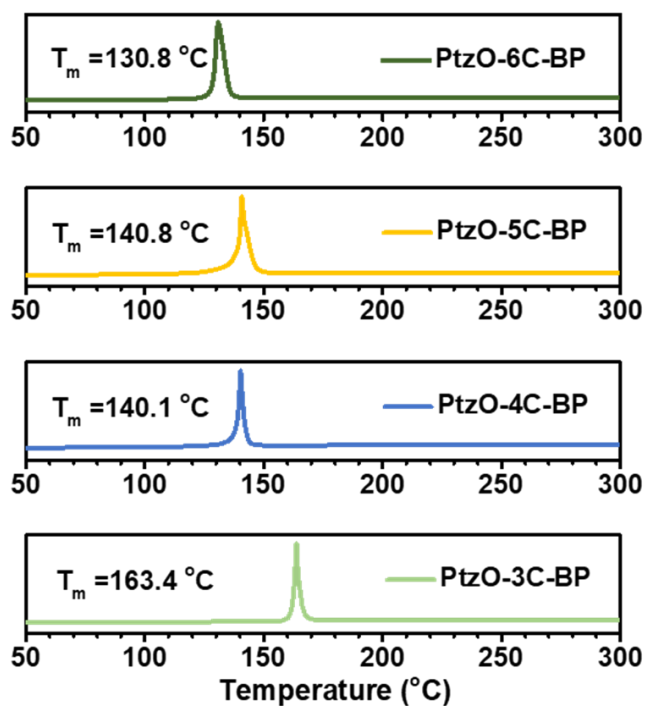
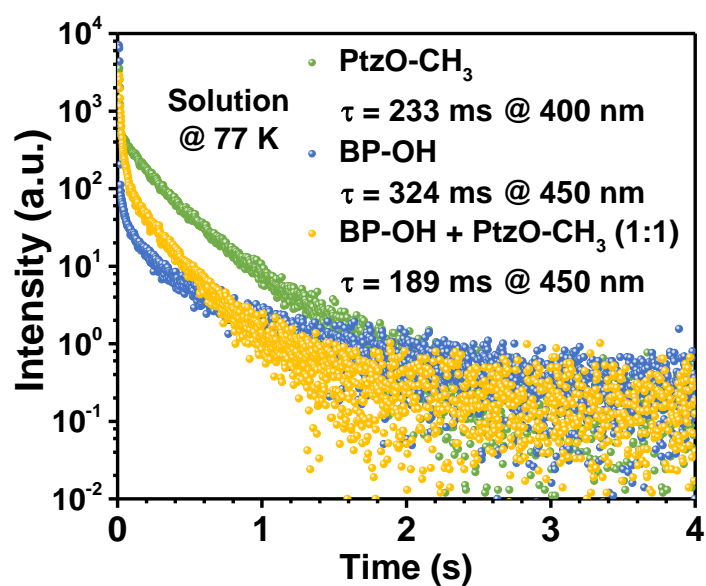


Figure S10 Thermo-gravimetric analysis (TGA) curves of Ptzo-nC-BP ( $n = 3-6$ ).



**Figure S11** Differential scanning calorimeter (DSC) curves of PtzO-nC-BP (n = 3-6).



**Figure S12** Phosphorescence decay curves of PtzO-CH<sub>3</sub>, BP-OH and PtzO-CH<sub>3</sub> + BP-OH (molar ratio 1:1) in solution state at 77 K ( $\lambda_{\text{ex}} = 330 \text{ nm}$ ,  $10 \mu\text{M}$ ).

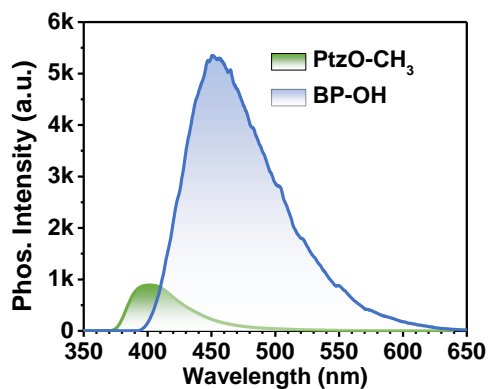


**Figure S13** Phosphorescence spectra of PtZO-CH<sub>3</sub> and BP-OH in solution state at 77 K ( $\lambda_{\text{ex}} = 330$  nm; 10  $\mu\text{M}$  same slit: ex5-em5).

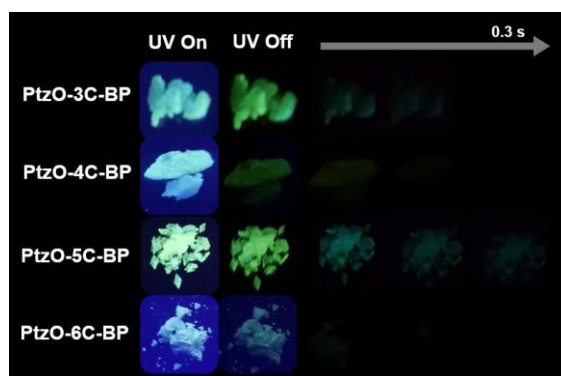


**Figure S14** Photographs of PtZO-nC-BP ( $n = 3-6$ ) taken at different times, before and after the removal of UV excitation.

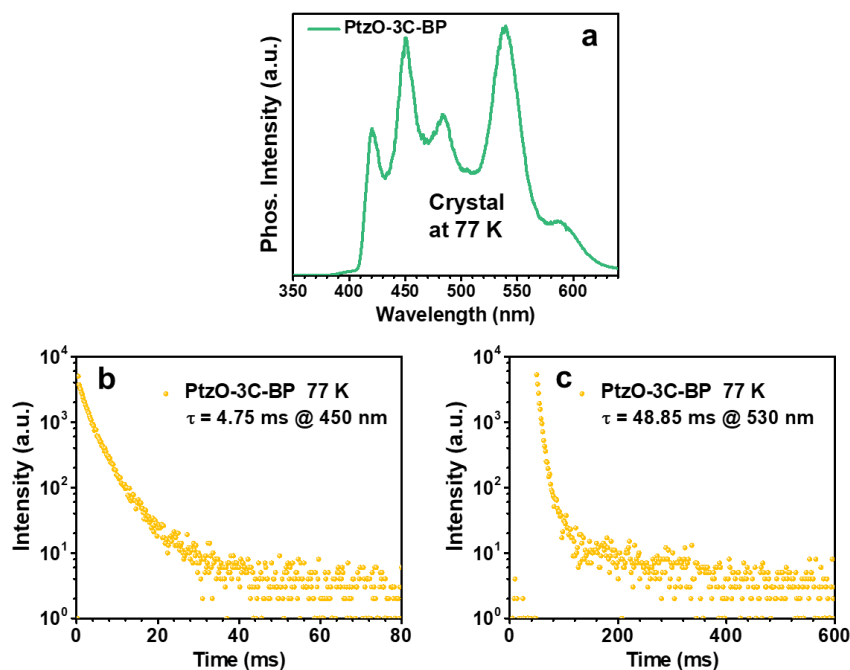


**Figure S15** (a) Phosphorescence spectra of PtZO-3C-BP crystal at 77 K ( $\lambda_{\text{ex}} = 330$  nm). (b) Phosphorescence decay curve of PtZO-3C-BP crystal at 450 nm under 77 K. (c) Phosphorescence decay curve of PtZO-3C-BP crystal at 530nm under 77 K.

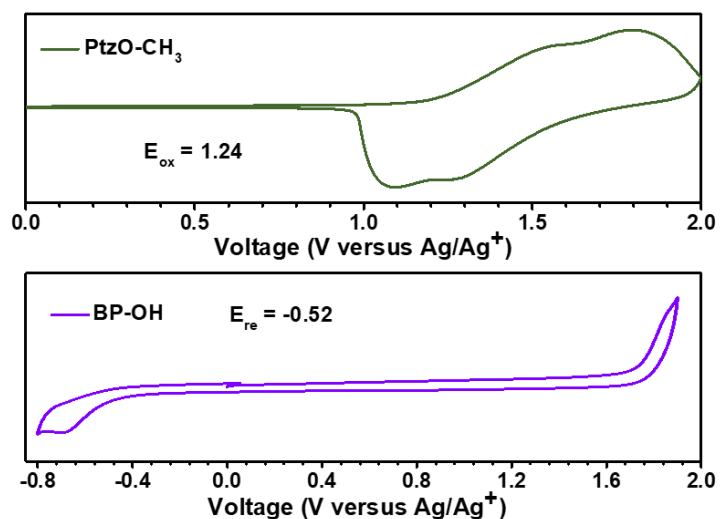


Figure S16 CV curves of Ptzo-CH<sub>3</sub> and BP-OH.

Table S1 Calculated energy levels of Ptzo-CH<sub>3</sub> and BP-OH

	Ptzo-CH <sub>3</sub>	BP-OH
HOMO (eV)	-5.60	-7.28
LUMO (eV)	-2.06	-3.84
$E_g$ (eV)	3.54	3.44
$E_{ox}$ or $E_{re}$ /V	1.24	-0.52
$\lambda_{onset}$ (nm)	350	360
$E_{(Fc/Fc^+)}/V$	0.44	

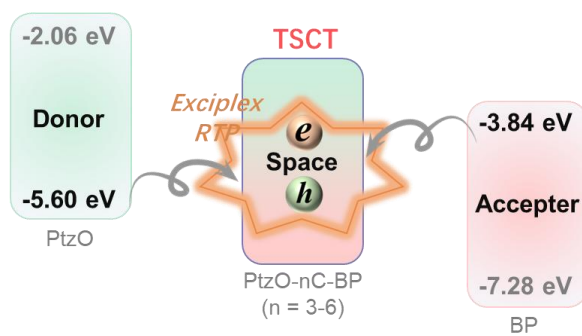
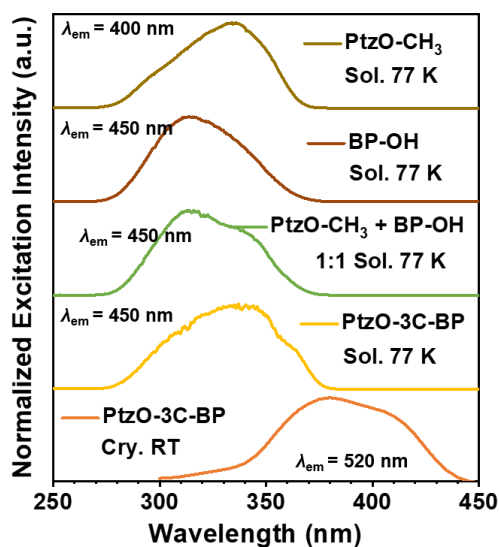
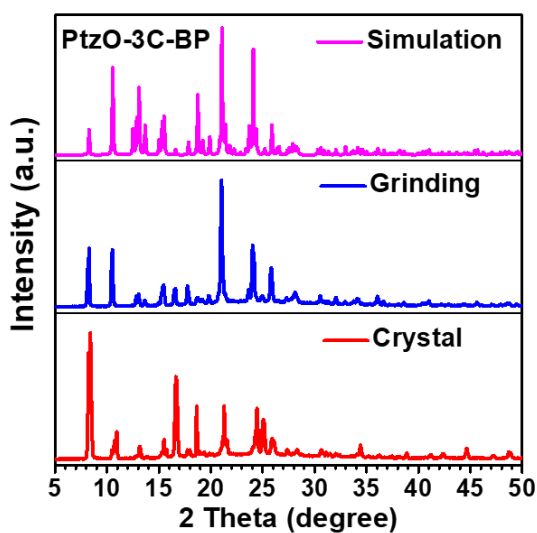


Figure S17 Schematic diagram of exciplex formation.



**Figure S18** Phosphorescence excitation spectra of Ptzo-CH<sub>3</sub>, BP-OH, their mixture and Ptzo-3C-BP in DCM solution states (10 μM) at 77 K and Ptzo-3C-BP in crystal state at room temperature.



**Figure S19** PXRD patterns for Ptzo-3C-BP in crystal state and grinding state, and simulation PXRD pattern based on its single crystal data, respectively.

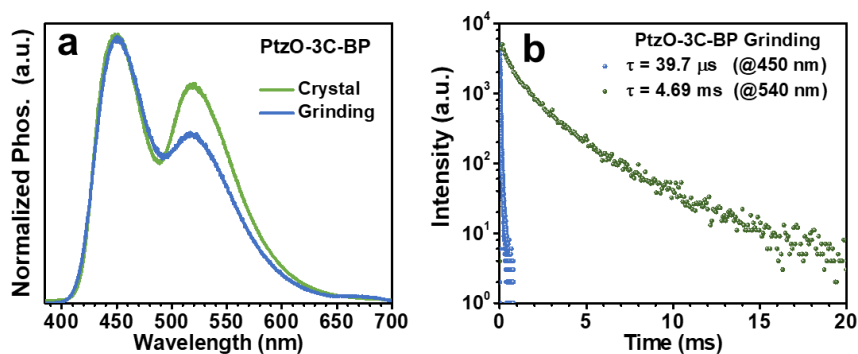


**Figure S20** (a) Phosphorescence spectra of Ptzo-3C-BP crystal before and after heavy grinding for 10 min at room temperature ( $\lambda_{\text{ex}} = 365 \text{ nm}$ ). (b) Phosphorescence decay curves of Ptzo-3C-BP crystal after heavy grinding for 10 min at room temperature ( $\lambda_{\text{ex}} = 365 \text{ nm}$ ). (Greater sensitivity of CT phosphorescence to molecular packing)



**Table S2** Single crystal structure data of PtzO-3C-BP.

Name	PtzO-3C-BP
Formula	C <sub>28</sub> H <sub>23</sub> N <sub>2</sub> O <sub>4</sub> S <sub>2</sub>
Wavelength(Å)	1.54184
Space Group	P n
Cell Lengths (Å)	a=8.1310(1); b=10.6646(2); c=13.5079(3)
Cell Angles (°)	α=90; β=91.796(2); γ=90
Cell Volume (Å <sup>3</sup> )	1170.75(4)
Z	2
Density (g/cm <sup>3</sup> )	1.332
F (000)	492
h <sub>max</sub> , k <sub>max</sub> , l <sub>max</sub>	9,12,16
CCDC Number	2088011

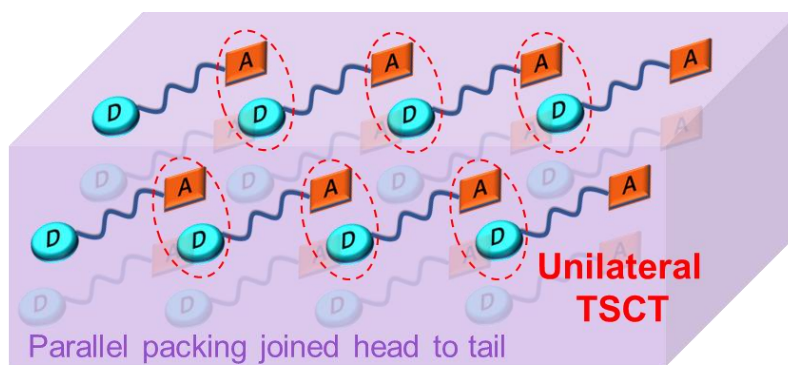


**Figure S21** Schematic illustration of D-A packing in PtzO-3C-BP crystal.

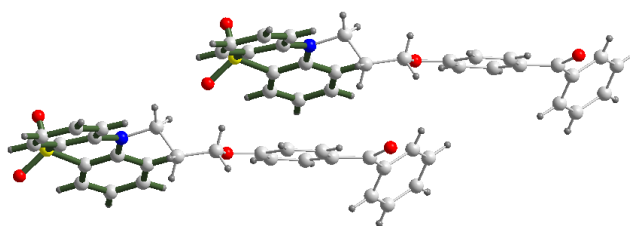


**Figure S22** Local packing of PtzO-3C-BP crystal, in which no  $\pi$ - $\pi$  stacking was formed by adjacent phenothiazine 5,5-dioxide units.

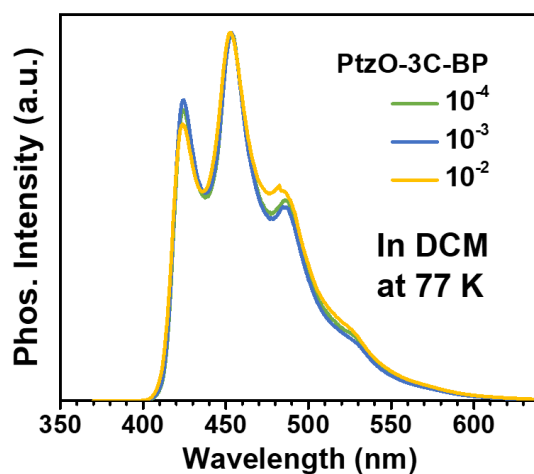


**Figure S23** Phosphorescence spectra of PtZO-3C-BP with different concentrations in DCM solution at 77 K ( $\lambda_{\text{ex}} = 330$  nm).

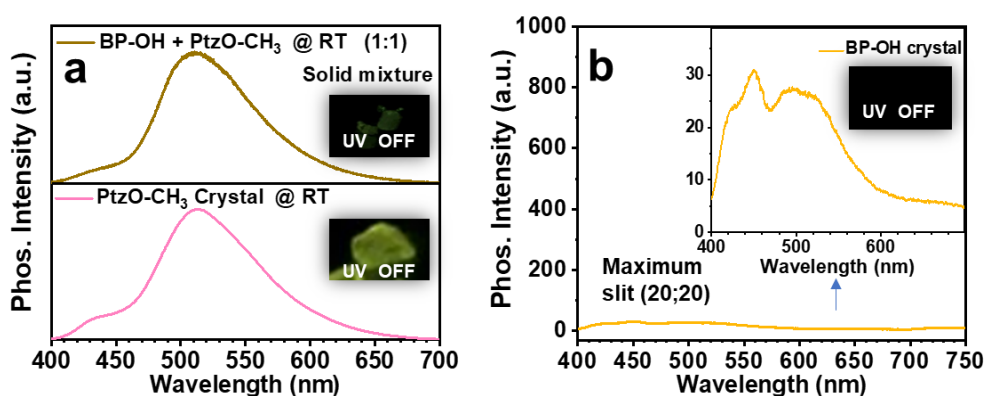


**Figure S24** (a) Phosphorescence spectra of PtZO-CH<sub>3</sub> + BP-OH solid mixture (molar ratio 1:1) and PtZO-CH<sub>3</sub> crystal and (b) BP-OH crystal at room temperature ( $\lambda_{\text{ex}} = 365$  nm).

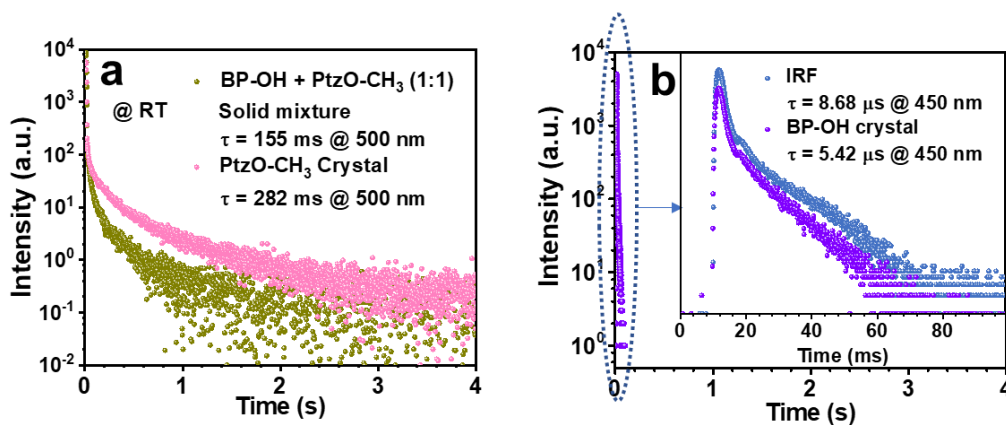


**Figure S25** (a) Phosphorescence decay curves of PtZO-CH<sub>3</sub> + BP-OH solid mixture (molar ratio 1:1) and PtZO-CH<sub>3</sub> crystal and (b) BP-OH crystal at room temperature ( $\lambda_{\text{ex}} = 365$  nm).

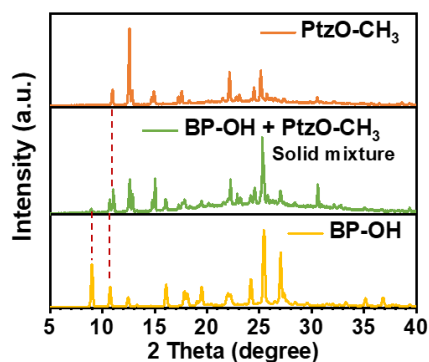


**Figure S26** PXR D patterns for Ptzo-CH<sub>3</sub> + BP-OH solid mixture and individual powders of Ptzo-CH<sub>3</sub> and BP-OH, respectively.

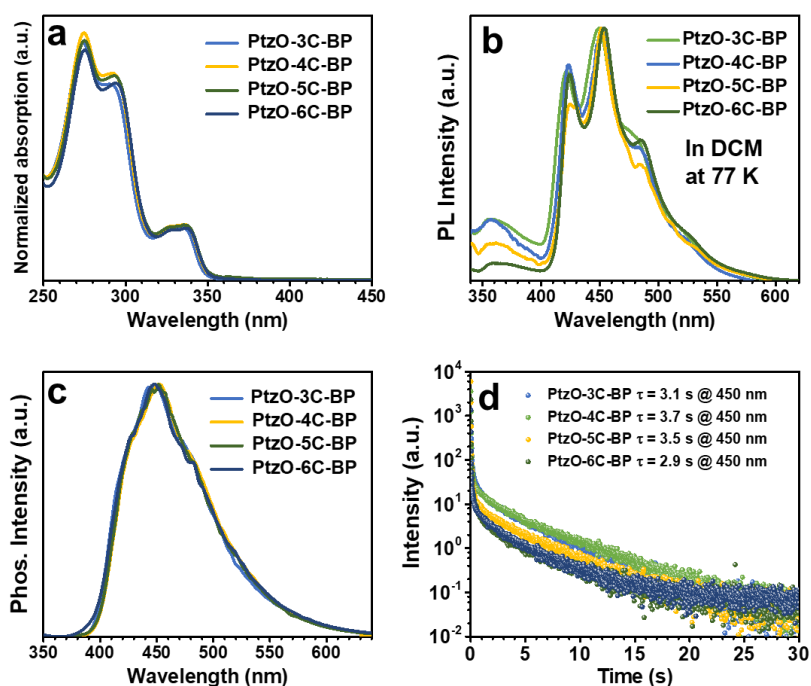


**Figure S27** (a) UV-Vis absorption spectra of Ptzo-nC-BP ( $n = 3-6$ ) in dichloromethane (DCM) solution ( $10 \mu\text{M}$ ). (b) Steady-state PL spectra of Ptzo-nC-BP ( $n = 3-6$ ) in DCM solution ( $10 \mu\text{M}$ ) at 77 K ( $\lambda_{\text{ex}} = 330$  nm). (c) Phosphorescence spectra of Ptzo-nC-BP ( $n = 3-6$ ) in DCM solution ( $10 \mu\text{M}$ ) at 77 K ( $\lambda_{\text{ex}} = 330$  nm). (d) Corresponding time-resolved phosphorescence decay curves of Ptzo-nC-BP ( $n = 3-6$ ) in DCM solution ( $10 \mu\text{M}$ ) at 77 K ( $\lambda_{\text{ex}} = 330$  nm).

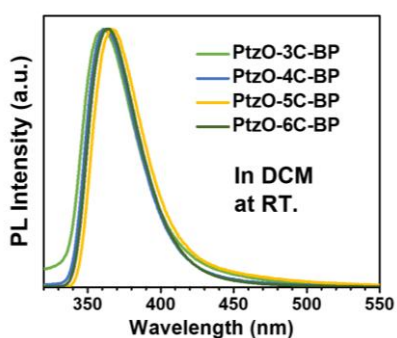


**Figure S28** Steady-state PL spectra of Ptzo-nC-BP ( $n = 3-6$ ) in DCM solution ( $10 \mu\text{M}$ ) at room temperature ( $\lambda_{\text{ex}} = 330$  nm).

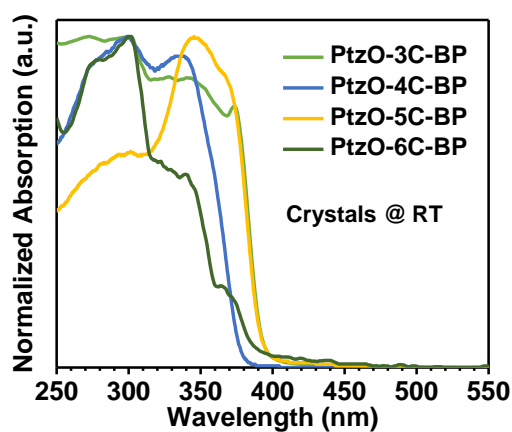


Figure S29 UV-Vis absorption spectra of PtzO-nC-BP (n = 4-6) in crystal state at room temperature.

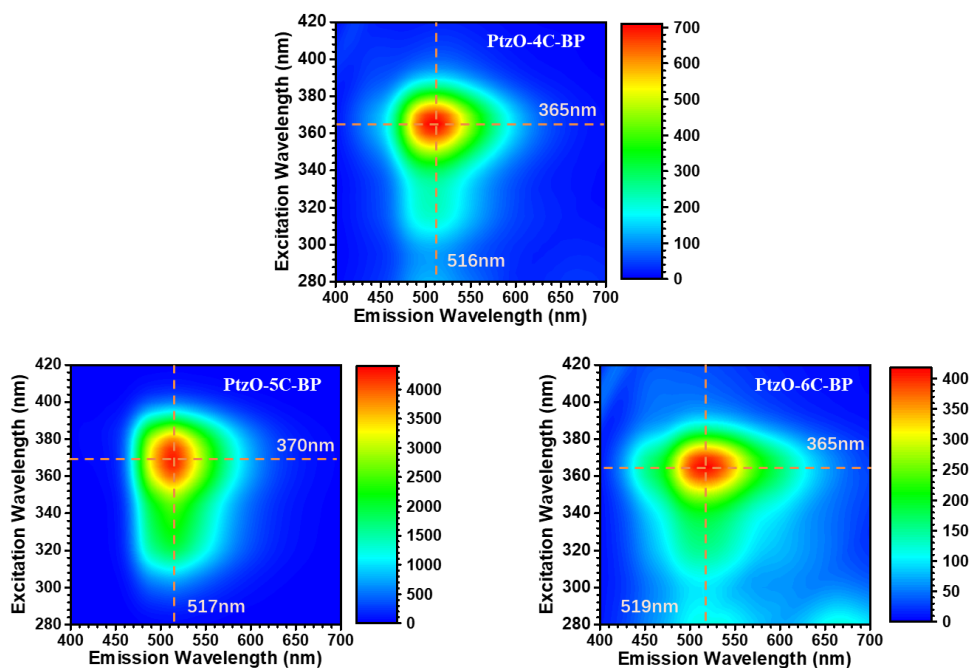


Figure S30 Excitation-phosphorescence mappings of PtzO-nC-BP (n = 4-6) in crystal state at room temperature.

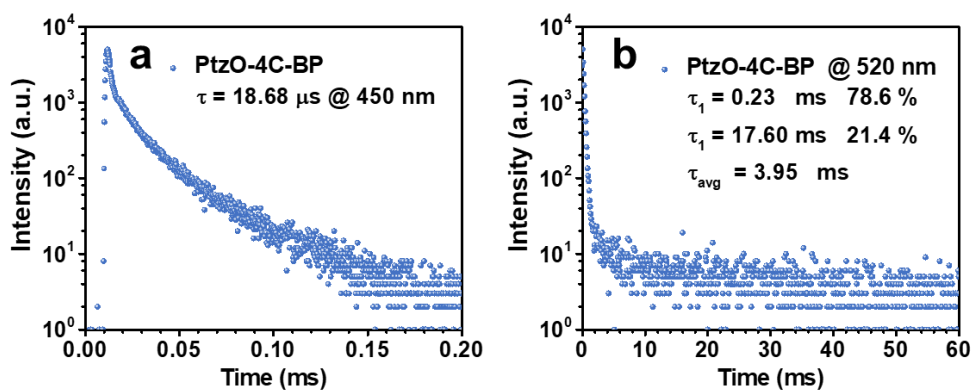
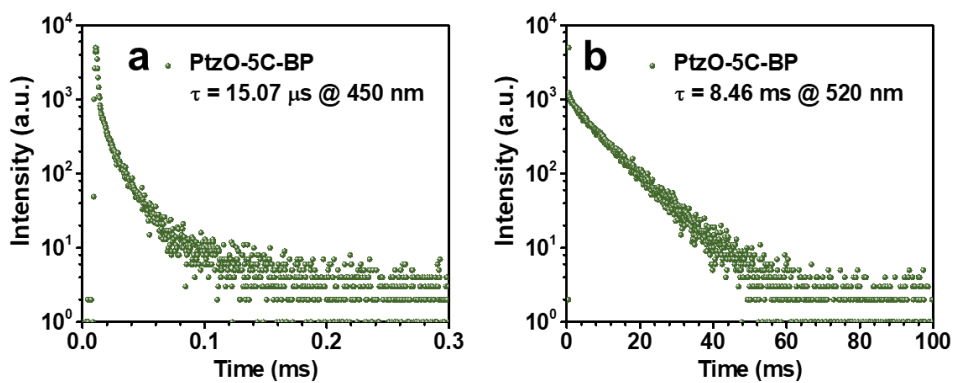
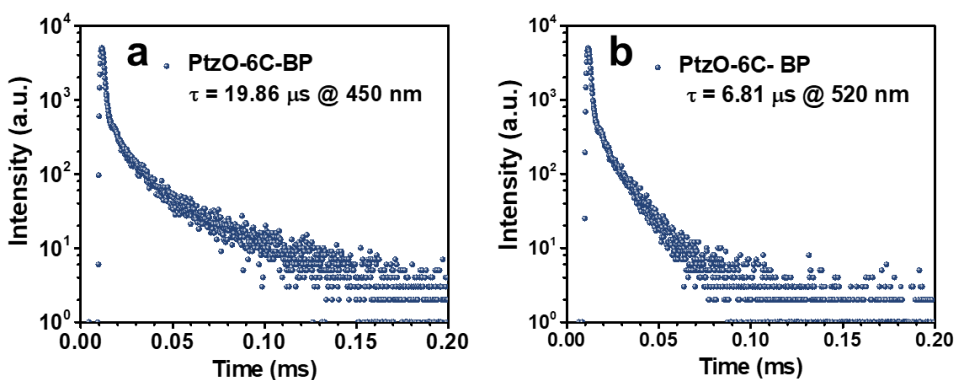


Figure S31 Time-resolved RTP decay curves of PtzO-4C-BP crystal at (a) 450 nm and (b) 520 nm ( $\lambda_{\text{ex}} = 365$  nm).



**Figure S32** Time-resolved RTP decay curves of PtzO-5C-BP crystal at (a) 450 nm and (b) 520 nm ( $\lambda_{ex} = 365$  nm).



**Figure S33** Time-resolved RTP decay curves of PtzO-6C-BP crystal at (a) 450 nm and (b) 520 nm ( $\lambda_{ex} = 365$  nm).

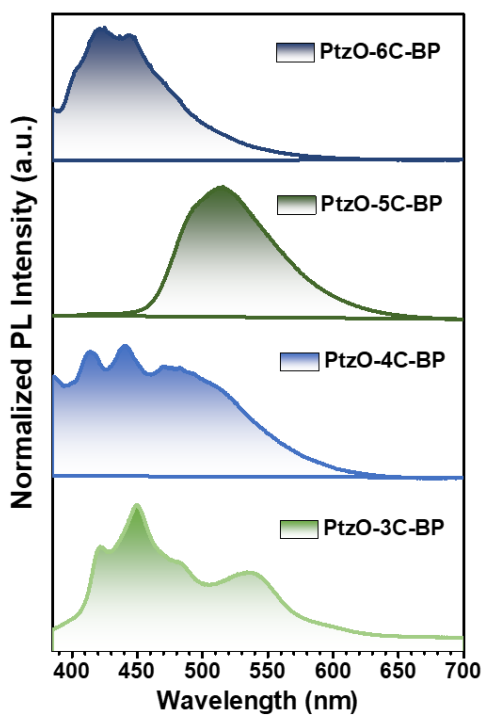


**Figure S34** Steady-state PL spectra of PtzO-nC-BP ( $n = 3-6$ ) in crystal state at room temperature.

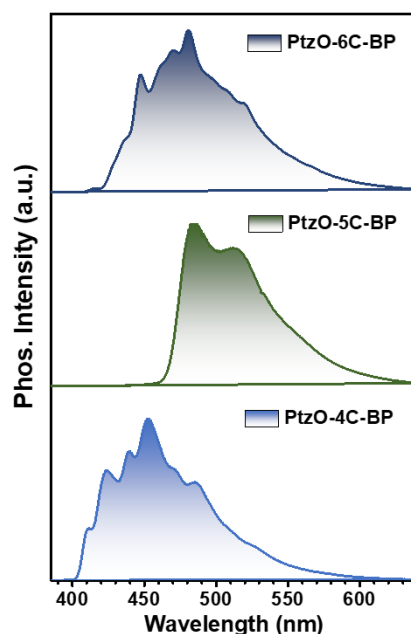


**Figure S35** Phosphorescence spectra of PtzO-nC-BP (n = 4-6) crystals at 77 K.

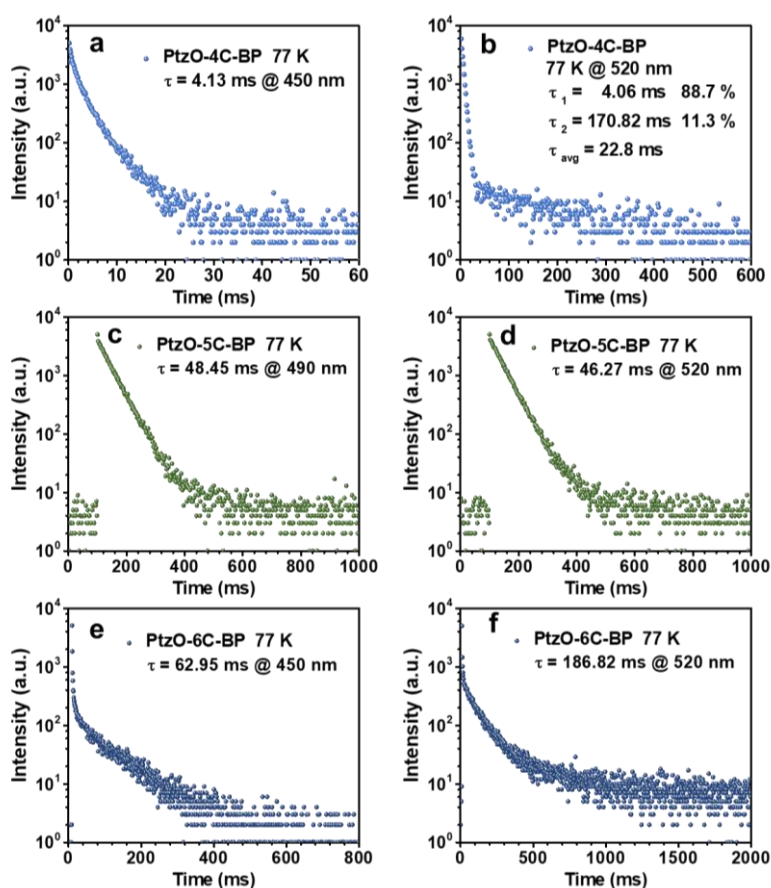


**Figure S36** (a) Phosphorescence decay curve of PtzO-4C-BP crystal at 450 nm under 77 K. (b) Phosphorescence decay curve of PtzO-4C-BP crystal at 530 nm under 77 K. (b) Phosphorescence decay curve of PtzO-5C-BP crystal at 450 nm under 77 K. (c) Phosphorescence decay curve of PtzO-5C-BP crystal at 530 nm under 77 K. (e) Phosphorescence decay curve of PtzO-6C-BP crystal at 450 nm under 77 K. (f) Phosphorescence decay curve of PtzO-6C-BP crystal at 530 nm under 77 K.

**Table S3** Single crystal data of PtzO-nC-BP (n = 4-6).

Name	PtzO-4C-BP	PtzO-5C-BP	PtzO-6C-BP
Formula	C <sub>29</sub> H <sub>25</sub> NO <sub>4</sub> S	C <sub>30</sub> H <sub>27</sub> NO <sub>4</sub> S	C <sub>31</sub> H <sub>29</sub> NO <sub>4</sub> S
Wavelength(Å)	1.54184	1.54184	1.54184
Space Group	P -1	P -1	-P 21/c
Cell Lengths (Å)	a = 7.9360(6) b = 11.6312(7) c = 14.689(1)	a = 8.1342(3) b = 10.9091(5) c = 14.7297(5)	a = 12.0408(2) b = 14.7040(3) c = 14.5910(2)
Cell Angles (°)	$\alpha$ = 106.507(6) $\beta$ = 105.371(7) $\gamma$ = 99.685(6)	$\alpha$ = 92.230(3) $\beta$ = 91.624(3) $\gamma$ = 107.461(4)	$\alpha$ = 90 $\beta$ = 94.545(2) $\gamma$ = 90
Cell Volume (Å <sup>3</sup> )	1209.21(17)	1244.80(9)	2575.18(8)
Z	2	2	4
Density (g/cm <sup>3</sup> )	1.328	1.328	1.32
F (000)	508	524	1080
h <sub>max</sub> , k <sub>max</sub> , l <sub>max</sub>	9,13,17	9,13,17	14,17,17
CCDC Number	2088093	2088010	2088094

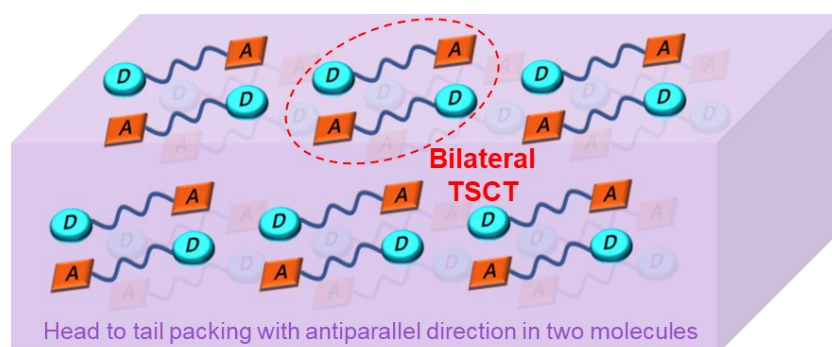


**Figure S37** Schematic illustration of D-A packing in PtzO-nC-BP (n = 4-6) crystals.

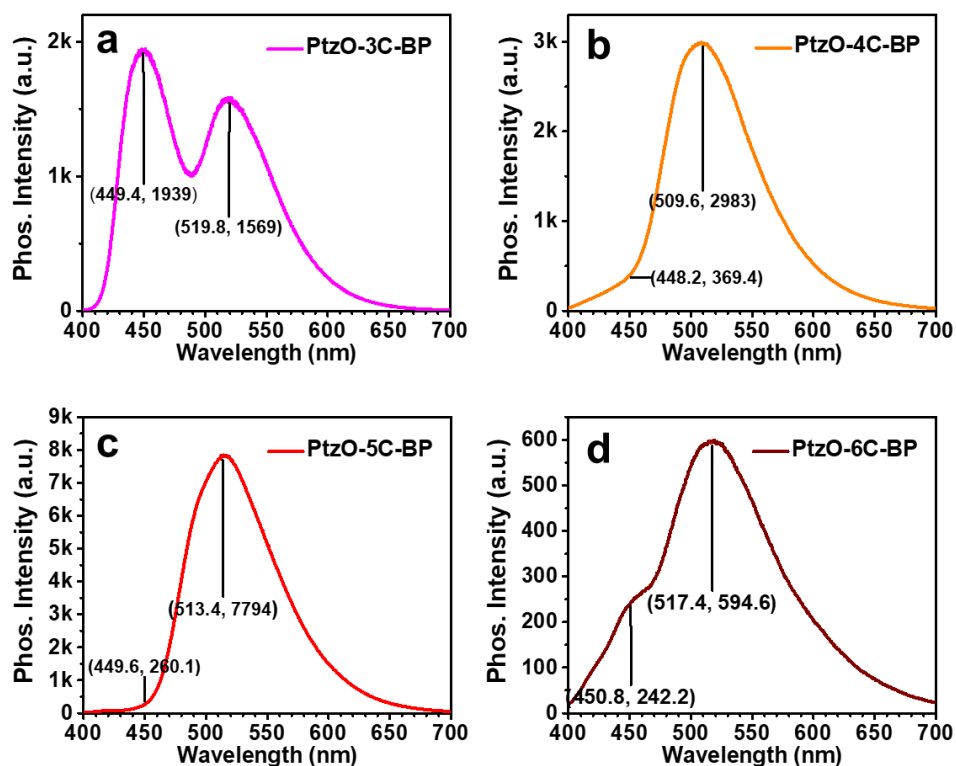


**Figure S38** The analyses of phosphorescence band and corresponding intensity of (a) PtzO-3C-BP crystal, (b) PtzO-4C-BP crystal, (c) PtzO-5C-BP crystal and (d) PtzO-6C-BP crystal at room temperature.

**Table S4** RTP performance of PtzO-nC-BP (n = 3-6) crystals at room temperature and the distance between N and O in D-A pairs.

	PtzO-3C-BP	PtzO-4C-BP	PtzO-5C-BP	PtzO-6C-BP
$I(^3\text{LE})$ (a.u.)	1939	369	260	242
$I(^3\text{CT})$ (a.u.)	1569	2983	7794	595
$I(^3\text{CT}) / I(^3\text{LE})$	0.8	8.1	30	2.5
$\tau(^3\text{LE})$ ( $\mu\text{s}$ )	53.8	18.7	15.1	19.9
$\tau(^3\text{CT})$ ( $\mu\text{s}$ )	5280	3950	8460	6.8
$\tau(^3\text{CT}) / \tau(^3\text{LE})$	98	212	560	0.34
$N-O$ ( $\text{\AA}$ )	5.00	4.99	4.67	5.63
$N-O^{-1}$ ( $\text{\AA}^{-1}$ )	1/5.00	1/4.99	1/4.67	1/5.63

$I(^3\text{LE})$  = the intensity of  $^3\text{LE}$  emission at around 450 nm;

$I(^3\text{CT})$  = the intensity of  $^3\text{CT}$  emission at around 520 nm;

$I(^3\text{CT}) / I(^3\text{LE})$  = the ratio of  $I(^3\text{CT})$  to  $I(^3\text{LE})$ ;

$\tau(^3\text{LE})$  = the lifetime of  $^3\text{LE}$  emission at around 450 nm;

$\tau(^3\text{CT})$  = the lifetime of  $^3\text{CT}$  emission at around 520 nm;

$\tau(^3\text{CT}) / \tau(^3\text{LE})$  = the ratio of  $\tau(^3\text{CT})$  to  $\tau(^3\text{LE})$ ;

$N-O$  = the distance between N and O in D-A pair;

$N-O^{-1}$  = the reciprocal of the distance between N and O in D-A pair.